NASA Technical Memorandum 106127

Composite Micromechanical Modeling Using the Boundary Element Method

Robert K. Goldberg and Dale A. Hopkins
Lewis Research Center
Cleveland, Ohio

Prepared for the
American Society for Composites Seventh Technical Conference on Composite Materials
sponsored by the American Society for Composites
University Park, Pennsylvania, October 13–15, 1992

NASA

COMPOSITE MICROMECHANICAL MODELING USING THE BOUNDARY ELEMENT METHOD

Robert K. Goldberg and Dale A. Hopkins
National Aeronautics and Space Administration
Lewis Research Center
Cleveland, Ohio 44135

SUMMARY

The use of the boundary element method for analyzing composite micromechanical behavior is demonstrated in this study. Stress-strain, heat conduction, and thermal expansion analyses are conducted using the boundary element computer code BEST-CMS, and the results obtained are compared to experimental observations, analytical calculations, and finite element analyses. For each of the analysis types, the boundary element results agree reasonably well with the results from the other methodologies, with explainable discrepancies. Overall, the boundary element method shows promise in providing an alternative method to analyze composite micromechanical behavior.

INTRODUCTION

In the analysis of composite materials, the behavior at the micromechanical (constituent) scale is often of interest. Several approaches have been used previously in examining micromechanical behavior. These include analytical methods, in which simplified models are used to yield closed form equations that describe effective composite properties, and some micromechanical responses (refs. 1 to 5). Discrete methods have also been used previously, in which representative volumes of fiber and matrix are modeled directly and analyzed (see ref. 6 as one of many examples). The finite element method (FEM) and boundary element method (BEM) are examples of discrete methods.

The objective of this study is to demonstrate the use of the boundary element method for analyzing composite micromechanical behavior as an alternative to other approaches. Specifically, composite micromechanical analyses have been conducted for several types of problems, and the boundary element results have been compared to those obtained from several other methodologies.

BACKGROUND

The boundary element method is a discrete analysis method in which discretized integral equations are solved over the surface of a domain. This methodology differs from the more familiar finite element method in which discretized differential equations are solved over the entire volume of a domain. By only requiring the surfaces of a domain to be discretized, the boundary element method can allow a significant reduction in the complexity and effort required for modeling.

To model a composite material, the outer surface of the matrix is discretized. To model the fibers, specially formulated "Insert Elements" (ref. 7) are used. For these insert elements, only the centerline of the fiber is defined, using nodes and elements, and the fiber radius is defined at each node. Both straight and curvilinear fibers are permitted. The fiber surfaces and the variation of the field variables in the plane of the fiber cross section are represented analytically within the boundary element formulation. To calculate the variation of the field variables along the length of the fiber, numerical integration is performed.

By using the boundary element method to model composite materials, efficiency (from a mesh discretization standpoint) can be significantly increased as compared to the finite element method. This

increase in efficiency is primarily due to the fact that the complexity of discretizing the interior of the domain is eliminated. By reducing the number of nodes and elements needed to model a problem, computational efficiency may also improve. However, due to the fact that commercial finite element codes are often optimized for a specific computer system, and the boundary element code that was used for this study is a research code, it is not reasonable at this point to compare computational efficiency.

The BEST-CMS (ref. 7) (Boundary Element Solution Technology-Composite Modeling System) computer code was used to conduct the boundary element analyses in this study. The analysis capabilities available within BEST-CMS include elastostatics, steady state and transient heat conduction, and steady state and transient thermoelastics. Several other capabilities of the code are worth mentioning. The fiber matrix interface can be idealized as a perfect bond, a linear spring interface, or a nonlinear spring-Coulomb-friction interface. The matrix material can be defined to have linear elastic or elastic-plastic constitutive behavior.

There are certain restrictions within the BEST-CMS computer code that should be noted. The analytical integration in the plane of the fiber cross section assumes that the fiber ends are not free surfaces, and thus exposed fiber ends cannot be represented. This restriction results in thermal and mechanical loads being transferred through the composite matrix to the end of the fiber. Also, the analytical integration of the fiber surface assumes that the fiber has a circular cross section. Particularly for angleplied composites, these restrictions result in the intersection of fibers with the matrix outer surface not being modeled correctly.

Finally, rigid plane (multi-point constraint) tying boundary conditions are not specifically available within BEST-CMS. To accommodate this limitation, either uniform displacements must be applied to nonrestrained faces of a model, or nodal averages of results must be taken over faces of interest in the computation of effective composite properties. Another consequence of this limitation is that for angleplied composites appropriate symmetry boundary conditions cannot be applied, and thus various nodal constraint boundary conditions must be applied in order to set bounds to the results.

MATERIAL SYSTEM

For the analyses in this study, a composite material system composed of SiC (SCS-6) fibers with a fiber diameter of 145 μm embedded within a titanium (Ti-15V-3Cr-3Sn-3Al or Ti-15-3 for short) matrix was used. The room temperature material properties of the constituents of the material are given in table I (ref. 8). A fiber volume fraction of 0.34 was used for the analyses.

Several important assumptions were applied to the material. Unless otherwise specified, residual stresses due to material processing and cooldown were not considered. In addition, a perfect bond was assumed between the fiber and matrix. Even though these assumptions do not apply to the actual material, the assumptions allowed the analysis to be simplified. In order to ensure that the assumptions remained valid, only linear deformations were considered, and the material was only loaded to a small percentage of failure strain. To simplify the thermal analyses, the material properties were assumed not to vary with temperature, which also is not the case with the actual material.

MODEL GENERATION

To generate the boundary element models for this study, a software interface to the commercial preprocessor PATRAN (ref. 9) was developed. This interface, titled COMGEN-BEM (Composite Model

Generation-Boundary Element Method) (ref. 10), enables the development of composite boundary element models based on user supplied:

- Fiber volume fraction
- Fiber diameter
- Model thickness
- Mesh density
- Material properties
- Fiber orientation angle
- Loads and boundary conditions

For this study, one-cell square and four-cell square three-dimensional boundary element models were used (fig. 1). The model thickness was set equal to the width. The four-cell square model was shown to give more accurate boundary element results, but the one-cell square model was used for cases where computational efficiency was more important. Eight noded quadrilateral elements are used to model the matrix outer surface, and three noded line elements are used to model the fiber elements.

It is important to note that the outer surface mesh topology shown in the figures is a mesh of the matrix only, not of the fibers. This topology for the matrix mesh was shown to give the most accurate results. Also, it should again be emphasized that only the outer surface of the composite matrix needed to be modeled. By representing the fibers with line elements, to model angleply composites the fiber line elements need only to be rotated. This procedure is much simpler than would be required for finite element modeling, where complex interior meshing would be required.

STRESS-STRAIN ANALYSES

The first set of analyses involved studying the stress-strain behavior of the SiC/Ti-15-3 material. A four-cell square model was used, and ply orientations of $[0]_8$, $[90]_8$, $[\pm 30]_{2s}$, and $[\pm 45]_{2s}$ were considered. The original boundary conditions included clamping the back face of the model, applying a uniform tensile stress to the front face of the model, and calculating the equivalent strain on the front face. Since the front face, as described before, cannot be defined as a rigid plane, the equivalent strain was calculated by taking the average of the nodal displacements and dividing that value by the model thickness. The stresses were applied up to the approximate point where the material behavior became nonlinear for each ply layup. The boundary element results were compared to experimental results obtained by Lerch and Saltsman (ref. 8) and, where possible, to results obtained from similar models by the finite element program NASTRAN (ref 11). First, the results from the stress-strain analyses for each ply layup are presented, followed by a discussion of the results.

The stress-strain results for the $[0]_8$ laminate are shown in figure 2. The BEST-CMS results are compared to both finite element and experimental results, and the material was loaded to approximately 44 percent of its failure strain. For this ply layup, the boundary element results are within 6.5 percent of the experimental results at the point of maximum discrepancy, and the finite element results are within 5 percent of the experimental results. Since the material was found to be linear up to a stress level of 900 MPa (ref. 8), the slight break seen in the experimental curve is most likely an experimental artifact.

The stress-strain results for the $[90]_8$ laminate, which was loaded to 11 percent of its failure strain, are shown in figure 3. The boundary element results are within 1.8 percent of the experimental results, while the finite element results are within 3.6 percent of the experimental. The break in the experimental curve is most likely due to the start of fiber/matrix debonding (ref. 8), which the analyses do not capture.

The stress-strain results for the $[\pm 30]_{2s}$ and the $[\pm 45]_{2s}$ laminates are shown in figures 4 and 5, respectively. The $[\pm 30]_{2s}$ laminate was loaded to 20 percent of its failure strain and the $[\pm 45]_{2s}$ laminate was loaded to less than 4 percent of its failure strain. Finite element results were not available for these layups, due to the complexity of developing finite element models for angleply laminates. The boundary element results for the $[\pm 30]_{2s}$ laminate were within 17.9 percent of the experimental results, and the boundary element results for the $[\pm 45]_{2s}$ laminate were within 10.6 percent of the experimental results.

To attempt to explain the discrepancy between the boundary element results and the experimental results, several further studies were conducted on the boundary element models for the $[0]_8$ and $[\pm 30]_{2s}$ laminates. First, the model was loaded with a cooldown from 700 to 21 °C to account for the residual stresses that were applied to the actual material (ref. 8) while maintaining the boundary condition of clamping the back face of the model. As can be seen in figures 6 and 7, adding residual stresses alone did not change the results for the linear range of the stress-strain curve. These results were somewhat expected since the experimental results were assumed to have zero stress and zero strain at the beginning of the test, thus neglecting any residual stresses. The residual stresses would probably become more significant if the fiber-matrix debonding behavior was being examined.

To examine the effects of the boundary conditions, the nodal constraint boundary condition was changed from clamping the back face to applying roller boundary conditions to the back, left and bottom faces of the four-cell square model. The cooldown to apply residual stresses was also applied to this problem. As can be seen in figures 6 and 7, changing the boundary conditions varied the results slightly for both ply orientations, thus serving to provide bounds on the results, but did not change the accuracy of the results to any significant extent.

Finally, the equivalent strain results for the clamped boundary condition with the thermal cooldown were examined on an interior face of the model, parallel to the front face, for both ply orientations. For this set of examinations, the boundary element results for the $[0]_8$ laminate improved as compared to the results obtained on the end face from within 6.5 percent of the experimental results to within 4.66 percent of the experimental results. For the $[\pm 30]_{2s}$ laminate, the boundary element results improved from within 17.9 percent of the experimental results to within 11.52 percent of the experimental results.

The reason for the improvement in the results on the interior faces is most likely due to the BEST-CMS assumption that the fiber ends are not free surfaces, thus not allowing exposed fiber ends to be represented. The assumption has two primary effects on the results on the end face. First, the loads must be transferred through the matrix to the end of the fiber, which can affect the end face results. Second, the results on the end face are the response of the matrix material only, while on the interior face the response of the fiber is more accurately represented. The fiber end assumption also helps to explain why the boundary element results for the $[0]_8$ laminate were less accurate than those for the $[90]_8$ laminate. Since the loading for the $[90]_8$ laminate is perpendicular to the fibers, the fiber end assumption probably plays a much less significant role for this laminate as compared to the $[0]_8$ laminate.

The $[0]_8$ and $[90]_8$ laminate results tended to be more accurate than the angleply laminate results. The discrepancy of results is most likely due to the BEST-CMS assumption that the fibers must have a circular cross section. The effect of this assumption is that for the angleply laminates, the length of the fiber must be cut off sufficiently far away from the outer surface of the matrix to assure a circular cross section. The reduction in fiber length causes a reduction in the effective fiber volume fraction, thus affecting the results. However, the effect of fiber/matrix debonding still needs to be examined, particularly for the angleply laminates. Including the debonding behavior will most likely improve the accuracy of all of the results, particularly at the higher strain levels, where the material nonlinearities become significant.

HEAT CONDUCTION ANALYSES

The second set of analyses involved examining the heat conduction capabilities of BEST-CMS, including both steady state and transient heat conduction. For these analyses, the SiC/Ti-15-3 was used as the base material. However, the constituent properties were assumed to not vary with temperature. Also, for the steady state heat conduction analyses, the thermal conductivity of the fiber was varied so that the ratio of fiber to matrix conductivities (K_f/K_m) ranged from 2.07 (base material) to 10.

For all of the heat conduction analyses, a unidirectional ply orientation was used. For the steady state problems, a four-cell square model was used. A one-cell square model was used for the transient problem in order to reduce the computation time. For the steady state problems, a 100 °C temperature gradient was imposed first parallel to the fibers (longitudinal case) and then perpendicular to the fibers (transverse case). The equivalent heat flux was then calculated on the low temperature face. The boundary element results were then compared to those obtained from NASTRAN finite element results and to results obtained from the Composite Cylinders analytical model (ref. 4). While experimental results would have been preferable to use as a baseline as opposed to an analytical model, experimental results were not available for this problem. For the transient analyses, a 100 °C temperature was applied to the back face of the model, and the equivalent temperature on the front face of the model was calculated as a function of time.

For the steady state heat conduction analyses, the equivalent heat flux is plotted as a function of the thermal conductivity ratio for the longitudinal case in figure 8 and for the transverse case in figure 9. For the longitudinal case, while the finite element results matched the theoretical results exactly, the boundary element results varied from the theoretical by 0.8 percent when the K_f/K_m ratio equaled 2, and by 21 percent when the K_f/K_m ratio equaled 10.

The cause of the discrepancy of the boundary element results, particularly at the higher conductivity values, is most likely related to the variation of the heat flux within each phase (fiber and matrix) that each method assumes. The finite element results showed, and the theory assumes, that the flux remains constant within each constituent, and is independent of the properties of the other constituents. For example, the flux values were constant within the matrix, and did not vary, even as the fiber conductivity was changed. The boundary element results, on the other hand, did show that the flux varied within each constituent and changed based on the changing of fiber properties. The variation within each phase became more pronounced as the fiber conductivity was increased, which accounts for the greater discrepancy of the results at higher fiber conductivities. Only by studying experimental results, however, can a true determination be made as to which method gives the most accurate answers.

For the transverse steady state heat conduction problem, the boundary element results were within 7.2 percent of the theoretical results, while the finite element results were within 4 percent of the theoretical results. The boundary element results were closer to the theoretical results at higher conductivity ratios than was seen in the longitudinal case. This increase in precision was probably due to the fact that for the transverse heat conduction, the continuity conditions (temperature and flux must remain constant across fiber/matrix boundaries) are the same for both the analytical theory and the boundary element method. This set of continuity conditions forces interaction between the constituents to be taken into account for all of the analysis methods.

For the transient heat conduction analyses, the equivalent temperature on the front face of the model is plotted as a function of time in figure 10. As can be seen in this figure, the temperature approaches an asymptotic value of 100 °C (the original applied temperature) as time is increased. This result is to be expected, as with no other boundary conditions applied the model should approach a constant steady state temperature.

THERMAL EXPANSION ANALYSES

The final set of analyses involved examining the thermal expansion behavior of the SiC/Ti-15-3 material system. The material properties of the constituents were assumed not to vary with temperature, and the fiber volume fraction was varied from 0.25 to 0.34 to 0.45. A one-cell square model with a unidirectional ply orientation was used. The back face of the model was clamped, a 100 °C temperature load was applied to the entire model, and the equivalent strain was calculated on the front face. The boundary element results were compared to NASTRAN results from equivalent finite element models, and to analytical results obtained from a rule of mixtures model (ref. 5). Again, while it would have been preferable to have experimental results to use as a baseline to compare the computational results against, due to the lack of experimental results an analytical model had to be utilized.

The equivalent strain on the front face is plotted as a function of the fiber volume fraction in figure 11. As can be seen from the figure, while the boundary element results and the finite element results are within 6.5 percent of each other, there is a significant discrepancy between these results and the theoretical results (around 35 percent for the boundary element models).

To explain these discrepancies, the case where the fiber volume fraction was 0.34 was further examined with additional boundary element analyses. First, the model was lengthened so that the thickness was equal to twice the model width. The discrepancy in strains was reduced to 17.45 percent as compared to the theory, which indicates that the original model was not long enough to eliminate the effects of applying the boundary conditions. By looking at a plane slightly on the interior of the model, the discrepancy in strains was reduced to 15.89 percent. The cause of the reduction in the discrepancy is probably due to the fact that the fiber ends in BEST-CMS cannot be free surfaces, as discussed before. Finally, the nodal constraints were changed for the longer model from clamping the back face to applying rollers to the back, bottom and left faces. With these boundary conditions, the strain discrepancy was reduced to 10 percent when the end face strains were examined and to 6 percent when the strains on an interior face were examined. The roller boundary condition allowed the model to expand freely in all three directions, which probably is a more accurate representation of the behavior, which yielded the more accurate results.

CONCLUSIONS

The boundary element code BEST-CMS was used to conduct composite micromechanical stress-strain, heat conduction, and thermal expansion analyses, with the results being compared to those obtained by alternate methodologies. For the stress-strain analyses, the original boundary element results were at most within 18 percent of the experimental results. The discrepancies were primarily due to the BEST-CMS assumptions that the fibers are not free surfaces and must have circular cross sections. For the heat conduction analyses, the boundary element results were found to differ from theoretical and finite element results due to BEST-CMS having fewer restrictions on the heat flux variation within a constituent phase. For the thermal expansion analyses, the boundary conditions and model length were found to have a significant effect on how close the boundary element results matched theoretical calculations. Overall, the specially formulated boundary element methods show promise in providing an alternative approach to analyzing composite micromechanical behavior.

Several areas of future work besides those mentioned already (applying fiber/matrix debonding to the stress-strain calculations, etc.) are being undertaken. First, efforts are ongoing to conduct analyses of woven composite materials. Due to the complex nature of this composite architecture, the advantages of the boundary element method model generation become even more significant in analyzing these materials.

Also, elastic-plastic matrix behavior will be incorporated into the stress-strain models, in order to more accurately capture the material behavior at high strain levels.

REFERENCES

1. Hopkins, D.A.; and Chamis, C.C.: A Unique Set of Micromechanics Equations for High Temperature Metal Matrix Composites. NASA TM-87154, 1985.

2. Aboudi, J.: Closed Form Constitutive Equations for Metal Matrix Composites. Int. J. Eng. Sci., Vol. 25, No. 9, 1987, pp. 1229–1240.

3. Weng, G.J.: Some Elastic Properties of Reinforced Solids, With Special Reference to Isotropic Ones Containing Spherical Inclusions. Int. J. Eng. Sci., Vol. 22, No. 7, 1984, pp. 845–856.

4. Christensen, R.M.: Mechanics of Composite Materials. John Wiley and Sons, 1979.

5. Tsai, S.W.; and Hahn, H.T.: Introduction to Composite Materials. Technomic Publishing Company, Inc., 1980.

6. Lerch, B.A.; Melis, M.E.; and Tong, M.: Experimental and Analytical Analysis of Stress-Strain Behavior in a $[90°/0°]_{2s}$, SiC/Ti-15-3 Laminate. NASA TM–104470, 1991.

7. Banerjee, P.K.; Henry, D.P.; Dargush, G.F.; and Hopkins, D.A.: BEST-CMS User's Manual, Version 2.0. Computational Engineering Mechanics Laboratory, Department of Civil Engineering, State University of New York at Buffalo, 1991.

8. Lerch, B.A.; and Saltsman, J.F.: Tensile Deformation Damage in SiC Reinforced Ti-15V-3Cr-3Al-3Sn. NASA TM–103620, 1991.

9. PATRAN Plus, Release 2.4, User Manual. PDA Engineering, 1989.

10. Goldberg, R.K.: COMGEN-BEM: Boundary Element Model Generation for Composite Materials Micromechanical Analysis. NASA TM–105548, 1992.

11. MSC/NASTRAN, Version 66, Vol. I and II, Users Manual. The MacNeil Schwendler Corporation, 1991.

TABLE I.—MATERIAL PROPERTIES FOR COMPOSITE CONSTITUENT MATERIALS

	SiC	Ti-15-3
Density, kg/m^3	2989.34	4760.81
Young's modulus, GPa	393	88
Poisson's ratio	0.19	0.32
Conductivity, W/mK	16.74	8.10
Heat capacity, J/kg K	1256.10	502.44
CTE, 1/°C	2.2×10^{-6}	8.1×10^{-6}

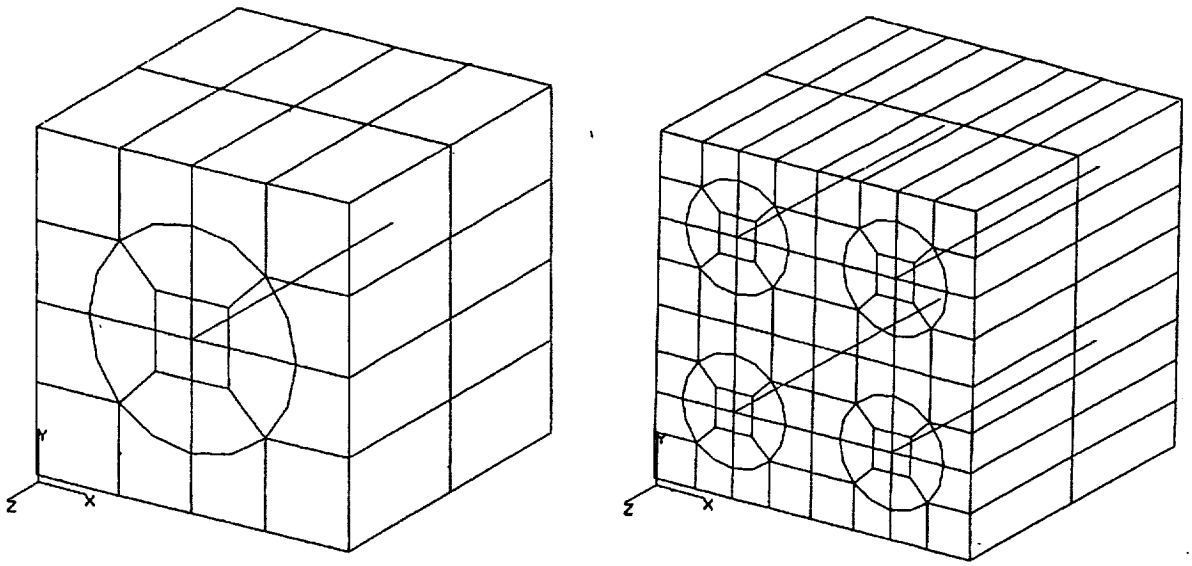

One cell square model. Four cell square model.

Figure 1.—COMGEN-BEM Boundary Element Models.

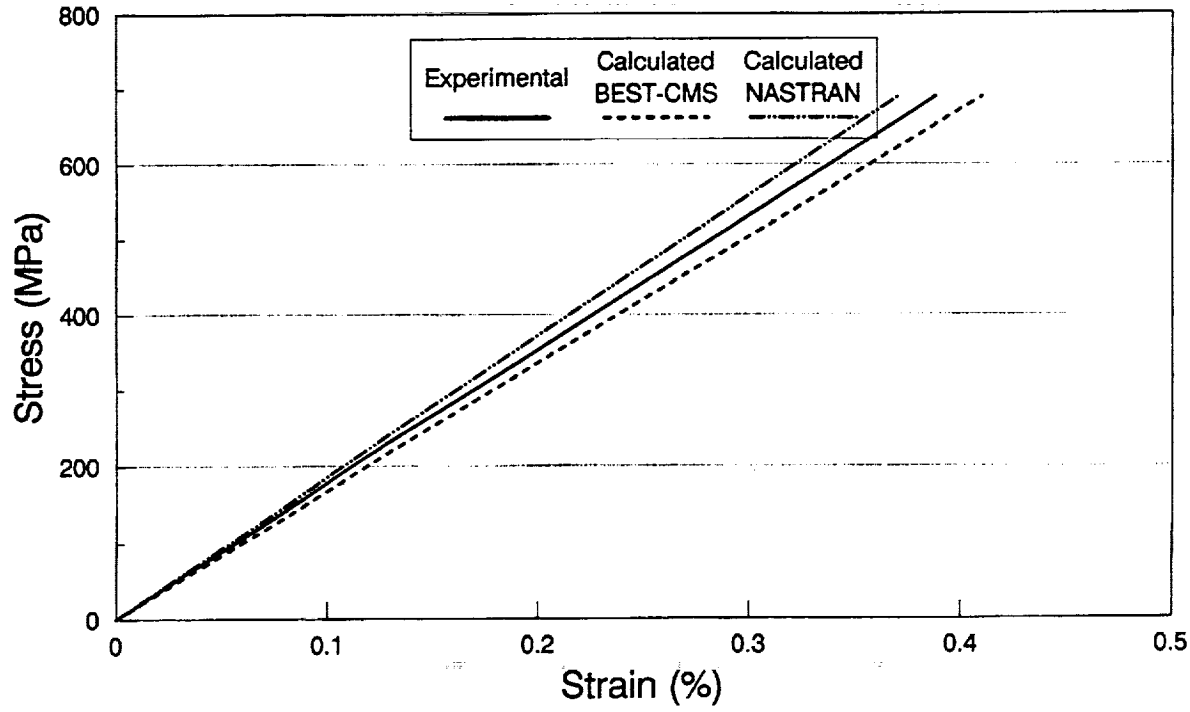

Figure 2.—Equivalent stress-strain for SiC/Ti-15-3 composite, $[0]_8$ laminate, FVR = 0.34, failure strain = 0.887%.

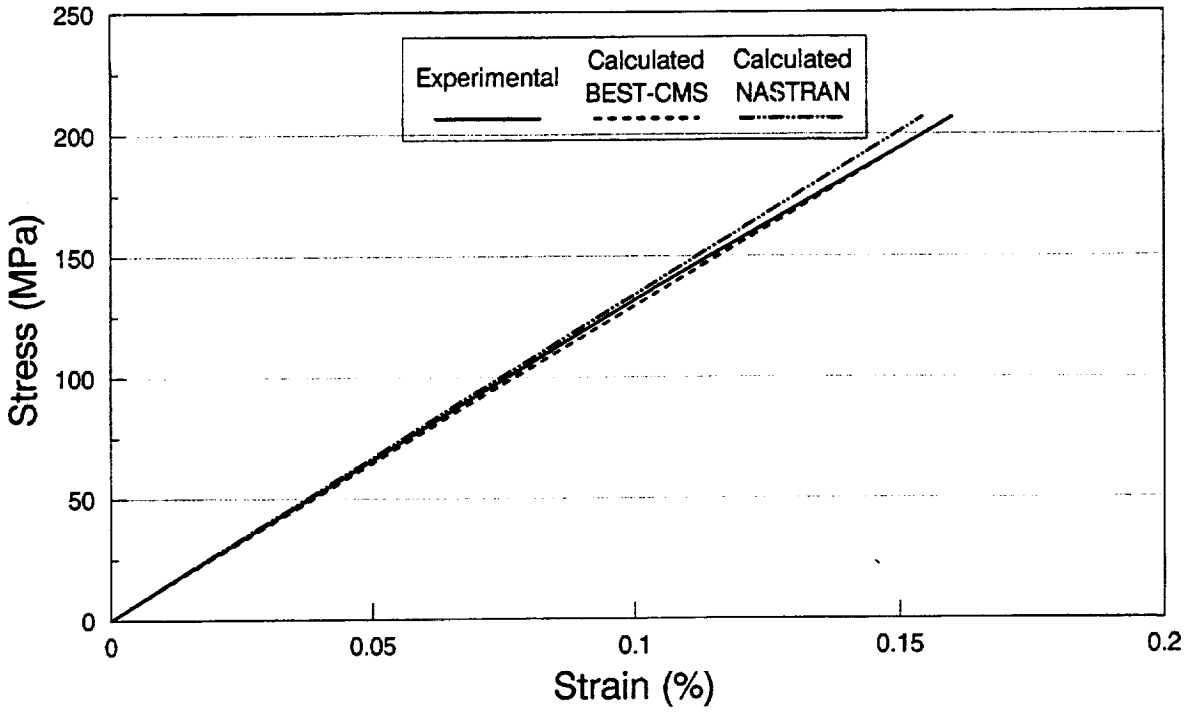

Figure 3.—Equivalent stress-strain for SiC/Ti-15-3 composite, $[90]_8$ laminate, FVR = 0.34, failure strain = 1.43%.

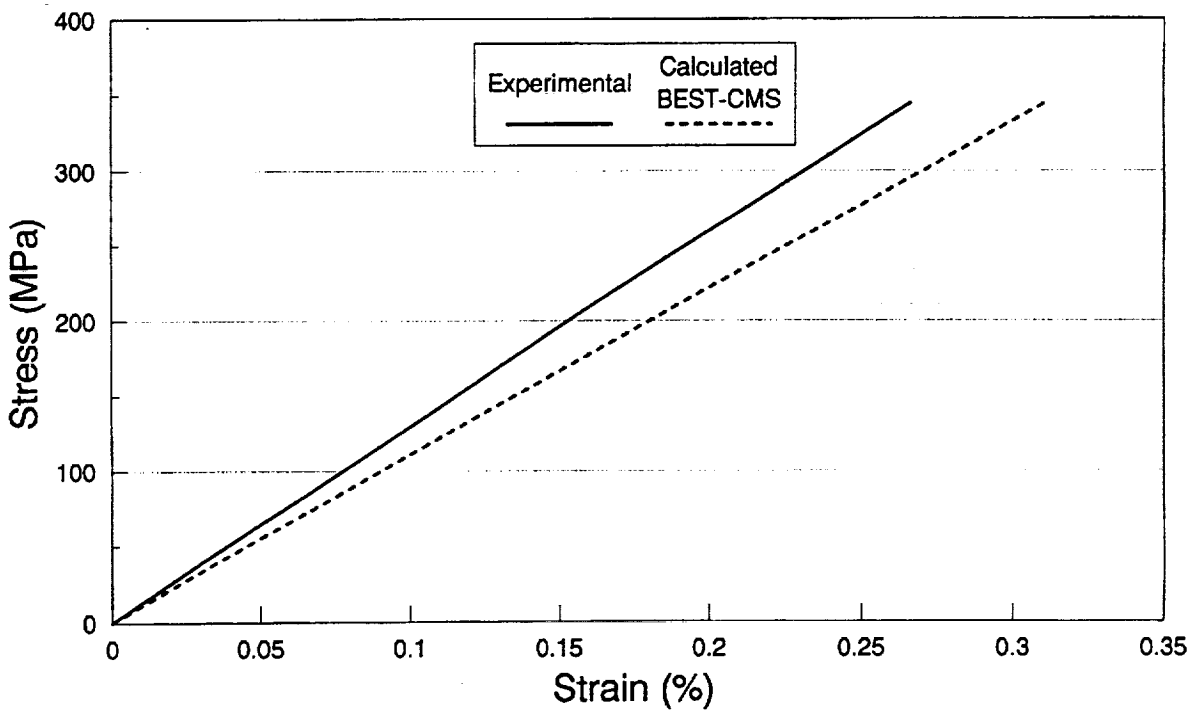

Figure 4.—Equivalent stress-strain for SiC/Ti-15-3 composite, $[+/-30]_{2s}$ laminate, FVR = 0.34, failure strain = 1.27%.

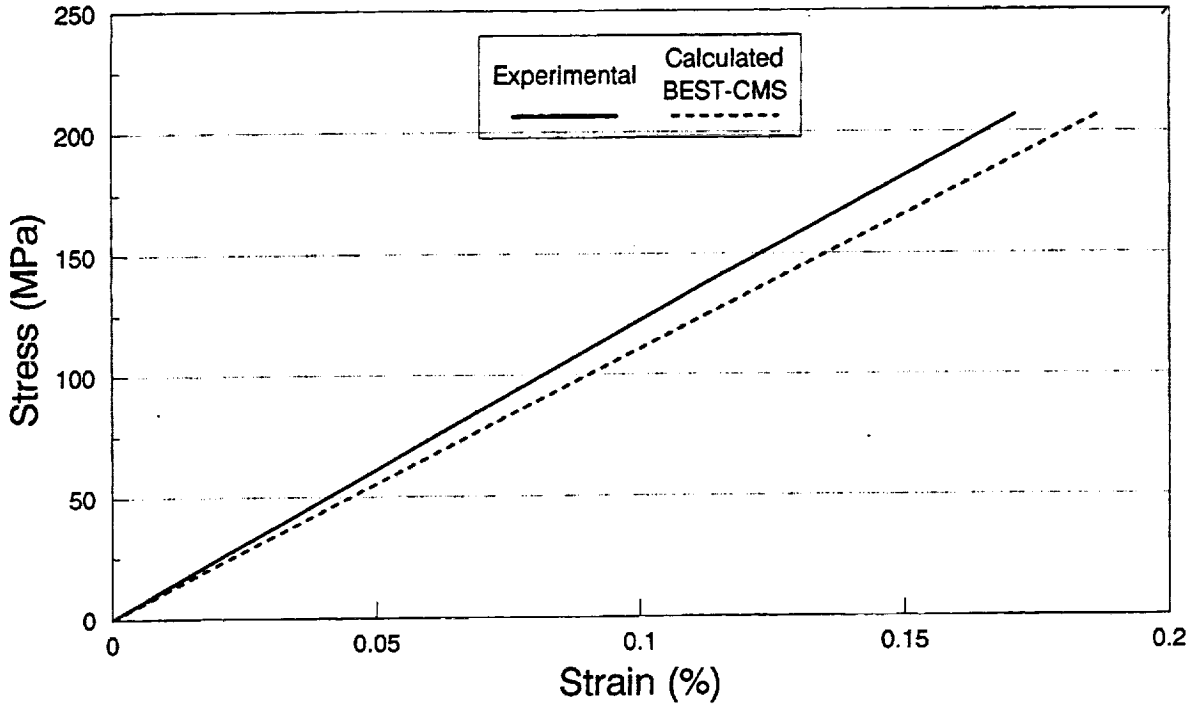

Figure 5.—Equivalent stress-strain for SiC/Ti-15-3 composite, $[+ / - 45]_{2S}$ laminate, FVR = 0.34, failure strain > 4.0%.

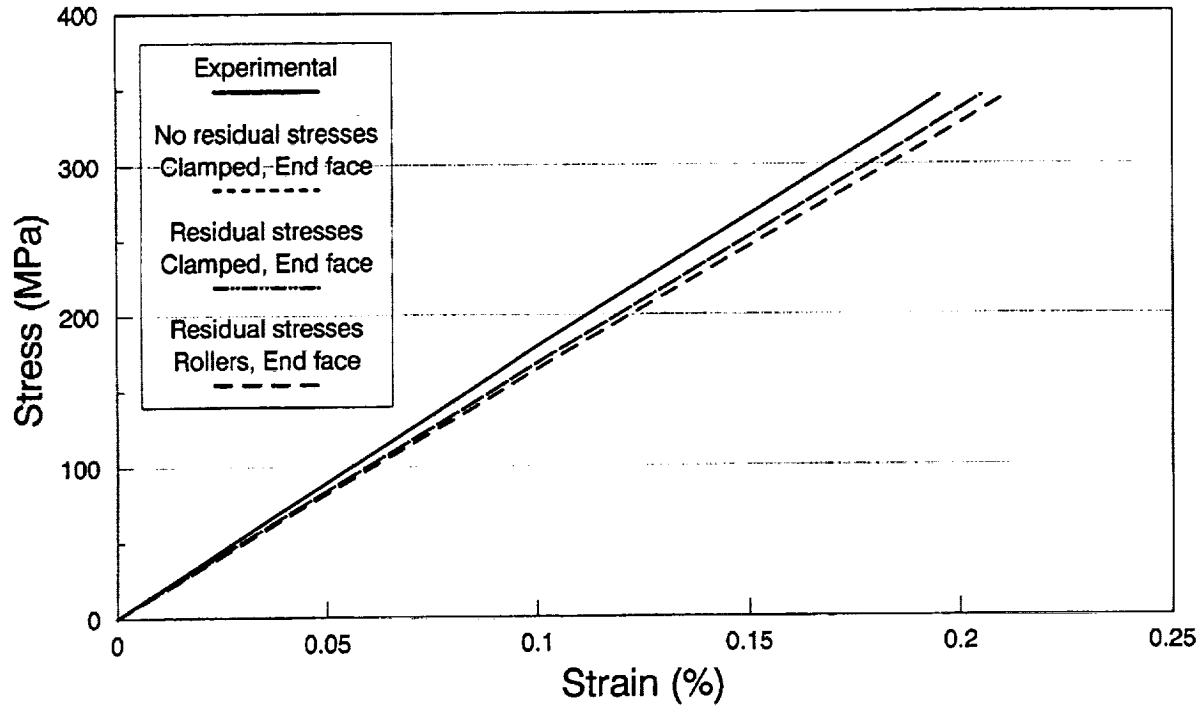

Figure 6.—Equivalent stress-strain for SiC/Ti-15-3 composite, $[0]_8$ laminate, FVR = 0.34, failure strain = 0.887%.

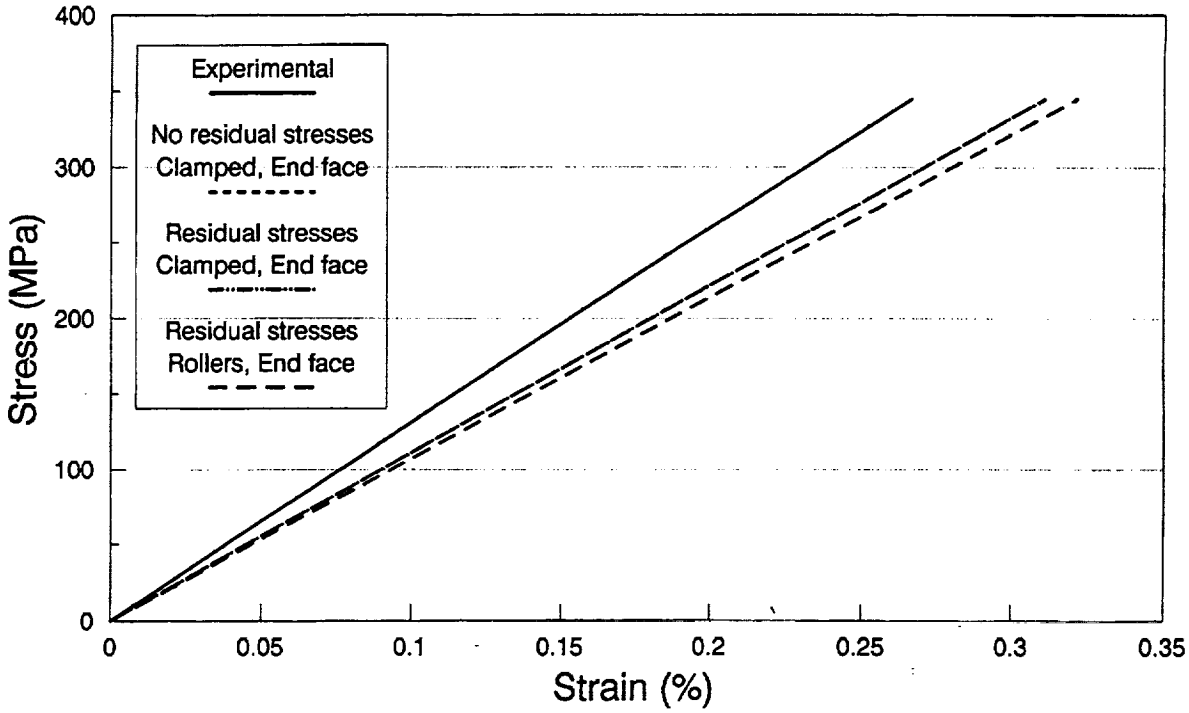

Figure 7.—Equivalent stress-strain for SiC/Ti-15-3 composite, $[+/-30]_{2s}$ laminate, FVR = 0.34, failure strain = 1.27%.

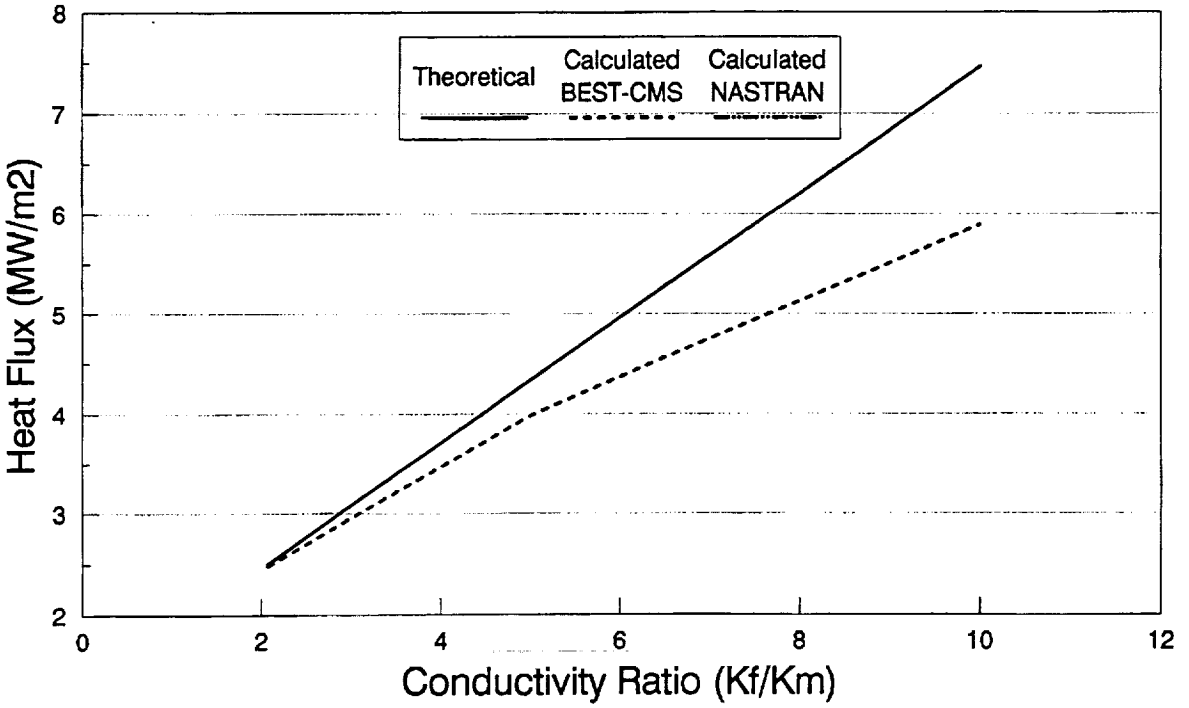

Figure 8.—Effect of fiber conductivity on longitudinal steady state heat flux, $[0]_8$ laminate, FVR = 0.34, temperature gradient = 100 deg. C, base material = SiC/Ti-15-3.

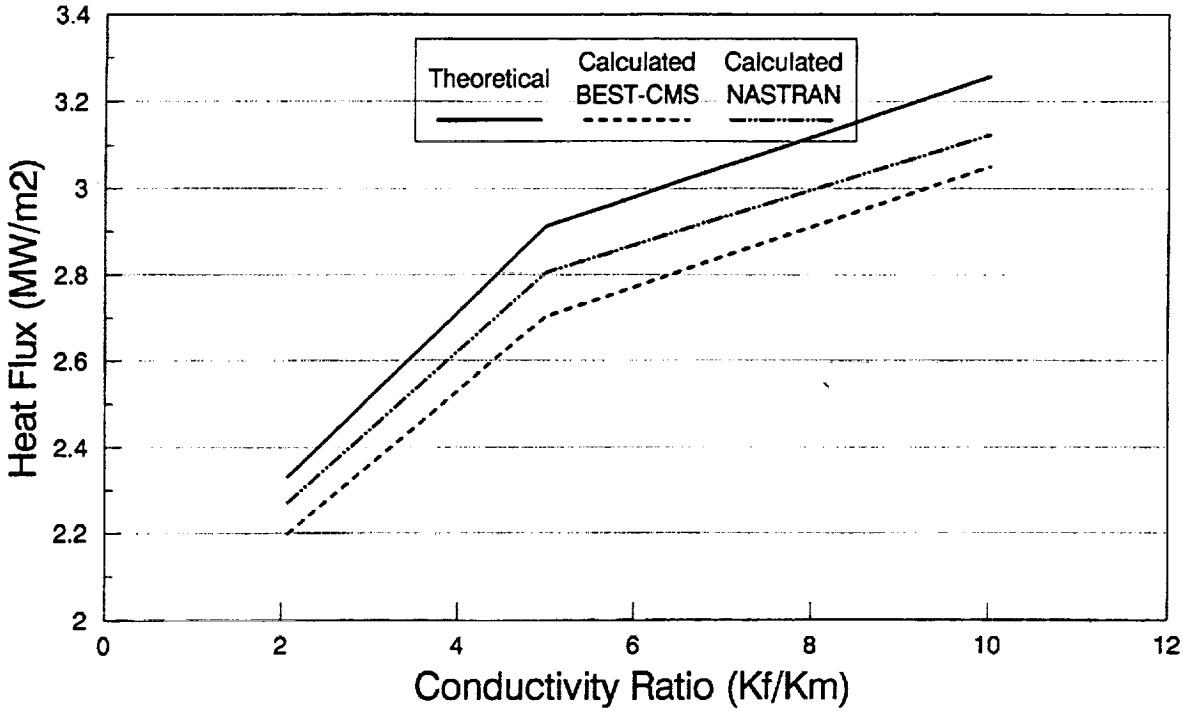

Figure 9.—Effect of fiber conductivity on transverse steady state heat flux, $[0]_8$ laminate, FVR = 0.34, temperature gradient = 100 deg. C, base material = SiC/Ti-15-3.

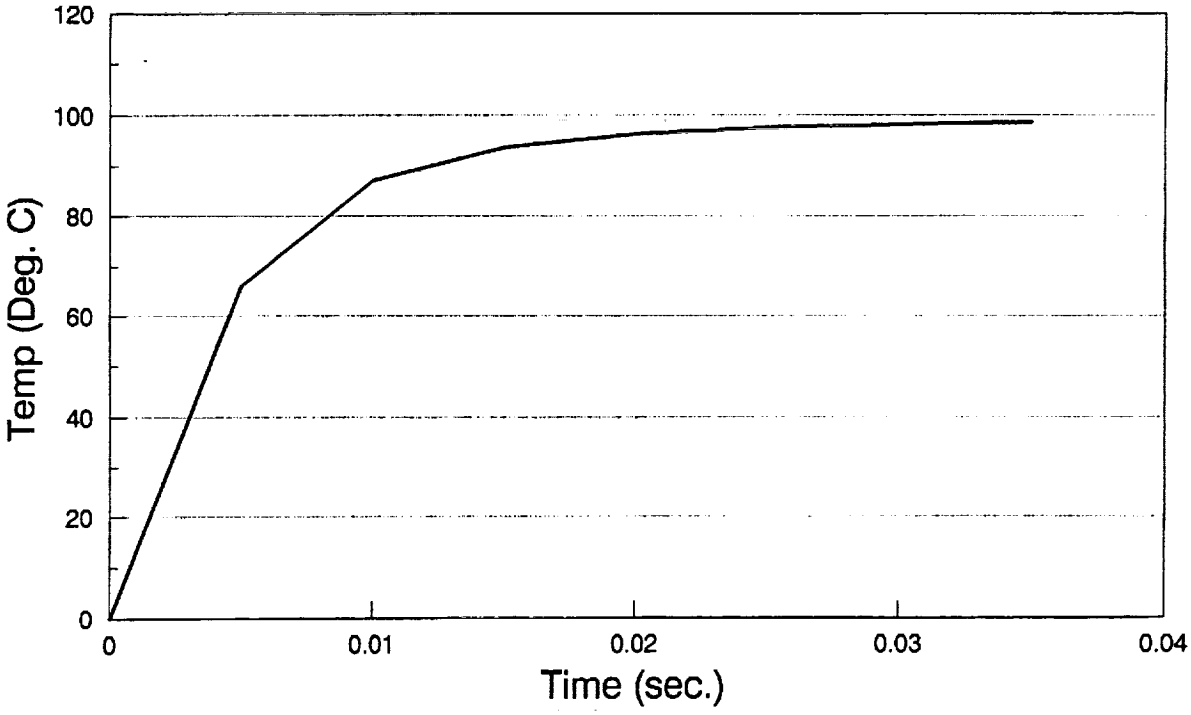

Figure 10.—Variation of equivalent temperature with time, $[0]_8$ laminate, FVR = 0.34, applied temp. = 100 deg. C, base material = SiC/Ti-15-3.

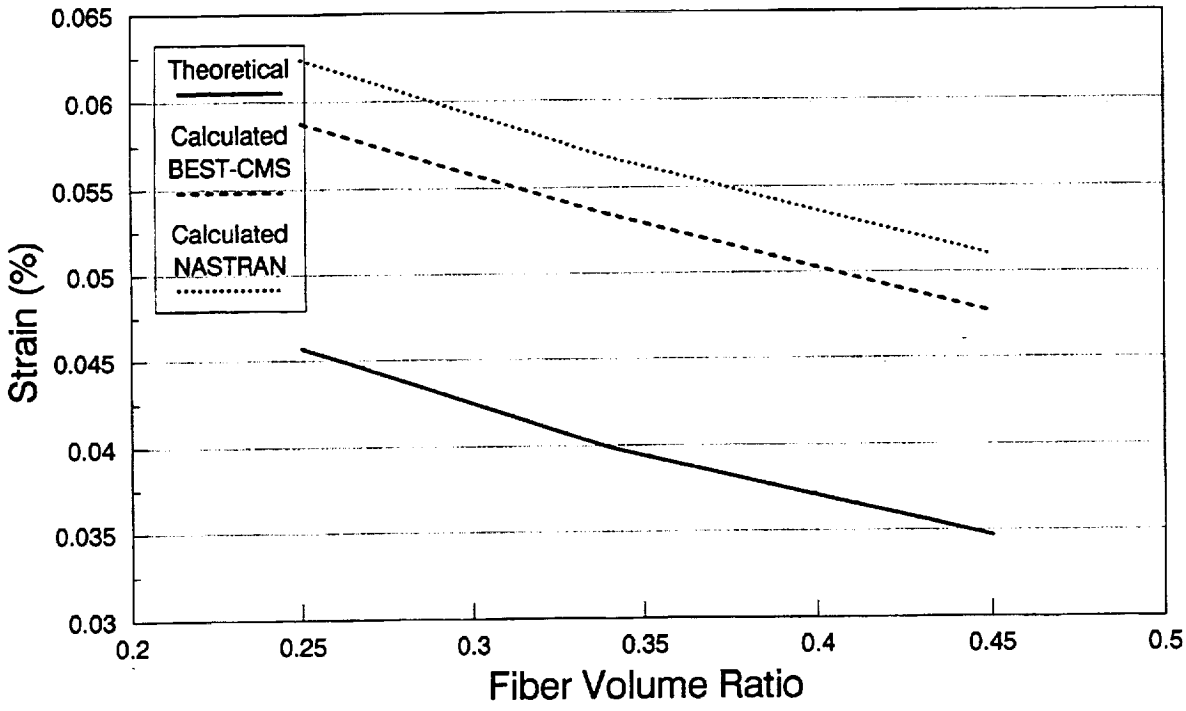

Figure 11.—Effect of FVR on equivalent longitudinal strain, $[0]_8$ laminate, temp. increase = 100 deg. C, base material = SiC/Ti - 15 - 3.

REPORT DOCUMENTATION PAGE

Form Approved
OMB No. 0704-0188

1. AGENCY USE ONLY (*Leave blank*)	2. REPORT DATE	3. REPORT TYPE AND DATES COVERED
	April 1993	Technical Memorandum

4. TITLE AND SUBTITLE

Composite Micromechanical Modeling Using the Boundary Element Method

5. FUNDING NUMBERS

WU-510-01-50

6. AUTHOR(S)

Robert K. Goldberg and Dale A. Hopkins

7. PERFORMING ORGANIZATION NAME(S) AND ADDRESS(ES)

National Aeronautics and Space Administration
Lewis Research Center
Cleveland, Ohio 44135-3191

8. PERFORMING ORGANIZATION REPORT NUMBER

E-7796

9. SPONSORING/MONITORING AGENCY NAME(S) AND ADDRESS(ES)

National Aeronautics and Space Administration
Washington, D.C. 20546-0001

10. SPONSORING/MONITORING AGENCY REPORT NUMBER

NASA TM-106127

11. SUPPLEMENTARY NOTES

Prepared for the American Society for Composites Seventh Technical Conference on Composite Materials sponsored by the American Society for Composites, University Park, Pennsylvania, October 13–15, 1992. Responsible person, Robert K. Goldberg, (216) 433–3330.

12a. DISTRIBUTION/AVAILABILITY STATEMENT

Unclassified - Unlimited
Subject Category 39

12b. DISTRIBUTION CODE

13. ABSTRACT (*Maximum 200 words*)

The use of the boundary element method for analyzing composite micromechanical behavior is demonstrated in this study. Stress-strain, heat conduction, and thermal expansion analyses are conducted using the boundary element computer code BEST-CMS, and the results obtained are compared to experimental observations, analytical calculations, and finite element analyses. For each of the analysis types, the boundary element results agree reasonably well with the results from the other methodologies, with explainable discrepancies. Overall, the boundary element method shows promise in providing an alternative method to analyze composite micromechanical behavior.

14. SUBJECT TERMS

Boundary element method; Composite materials; Finite element method

15. NUMBER OF PAGES

14

16. PRICE CODE

A03

17. SECURITY CLASSIFICATION OF REPORT	18. SECURITY CLASSIFICATION OF THIS PAGE	19. SECURITY CLASSIFICATION OF ABSTRACT	20. LIMITATION OF ABSTRACT
Unclassified	Unclassified	Unclassified	